Factors Affecting the Conformational Preference and Magnetic Shielding of Isobutenylene Chains in Macrocyclic Salicylideneaniline Derivatives

Hirohiko Houjou,*,# Seiji Tsuzuki, Yoshinobu Nagawa, Masatoshi Kanesato, and Kazuhisa Hiratani†,##

Nanoarchitectonics Research Center, National Institute of Advanced Industrial Science and Technology (AIST), Tsukuba Central 4, 1-1-1 Higashi, Tsukuba, Ibaraki 305-8562

†Department of Applied Chemistry, Utsunomiya University, 7-1-2 Youtou, Utsunomiya 321-8585

Received July 3, 2003; E-mail: h-houjou@aist.go.jp

The ^{1}H NMR chemical shifts and X-ray crystal structures of various salicylideneaniline derivatives containing an isobutenylene (2-methylenepropane-1,3-diyl) chain were analyzed in detail. In solution, these compounds were present to some extent as *syn–syn* conformers with respect to the isobutenylene chain; the actual *syn–syn* population depended on the molecular structure, especially on the size of the macrocycle. Small substituents on the phenyl ring hardly affected the stability of the *syn–syn* form at all, whereas replacement of the phenyl group with a naphthalene moiety considerably destabilized the *syn–syn* form relative to the *syn*–skew form. The conformation–chemical shift relationship was validly maintained irrespective of the substituent, provided the conformational preference was correctly taken into account.

Macrocyclic and macroacyclic Schiff bases have been extensively employed as ligands for mono- or multinuclear metal complexes, which are applicable to biomimetic catalysts, transport reagents, magnetic or electronic functional materials, building materials in nano-space construction and so on.[1–8] The ligands must be sophisticatedly designed so that their preferred conformation is appropriate for the desired complexation and architecture, especially in the integrated systems such as helicates which are accomplished by self-assembly.[9] Recently, we reported on several dinuclear metal complexes of salicylaldoimine ligands containing the isobutenylene (2-methylenepropane-1,3-diyl; Fig. 1a) chain.[10–12] These complexes exhibit helicate, meso-helicate, and tripodal cage structures, where the isobutenylene chains play a key role in regulating the three-dimensional structure. For example, the helicate complexes have the isobutenylene chain in skew–skew form (Fig. 1b, I), while the meso-helicate complexes have *syn*–skew form (Fig. 1b, II).[12,13] Inspired by this conformational variation, we could also propose a molecular system convertible between helicate and meso-helicate in response to an environmental change.

Now, we continue the study of the various complexes which show characteristic architecture and properties depending on the conformation of the isobutenylene chains. While the introduction of various substituents, including the replacement of aromatic rings, may fine-tune the properties, their effects on the conformational preference need to be clarified. Furthermore, it is suggested that a proper conformation of isobutenylene chain is crucial for the efficient synthesis of rotaxane that has been recently developed by Hiratani et al.[14] It is thus important to know the conformational preference of isobutenylene chains in a given chemical structure.

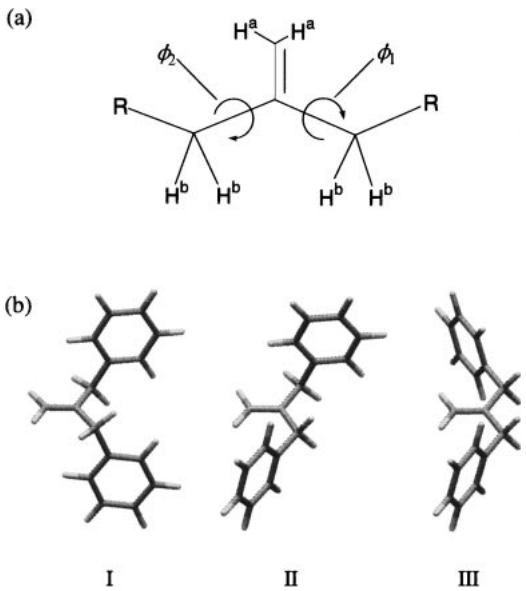

Fig. 1. (a) Designation of protons (H^a and H^b) and dihedral angles (ϕ_1 and ϕ_2) in the isobutenylene chain. (b) Three conformers grouped by the dihedral angles (ϕ_1, ϕ_2): I, skew–skew ($\phi_1 \sim 110°$, $\phi_2 \sim 110°$); II, *syn*–skew ($\phi_1 \sim 110°$, $\phi_2 \sim 0°$); and III, *syn–syn* ($\phi_1 \sim 0°$, $\phi_2 \sim 0°$).

In a previous study, we demonstrated that the ^{1}H NMR signals of H^a and H^b (Fig. 1a) of macrocyclic salicylideneaniline derivatives appear within a limited region corresponding to each conformer of the isobutenylene chains found in the X-

Present address: Institute of Industrial Science, University of Tokyo, 4-6-1 Komaba, Meguro, Tokyo 153-8505

AIST

Published on the web December 15, 2003; DOI 10.1246/bcsj.76.2405

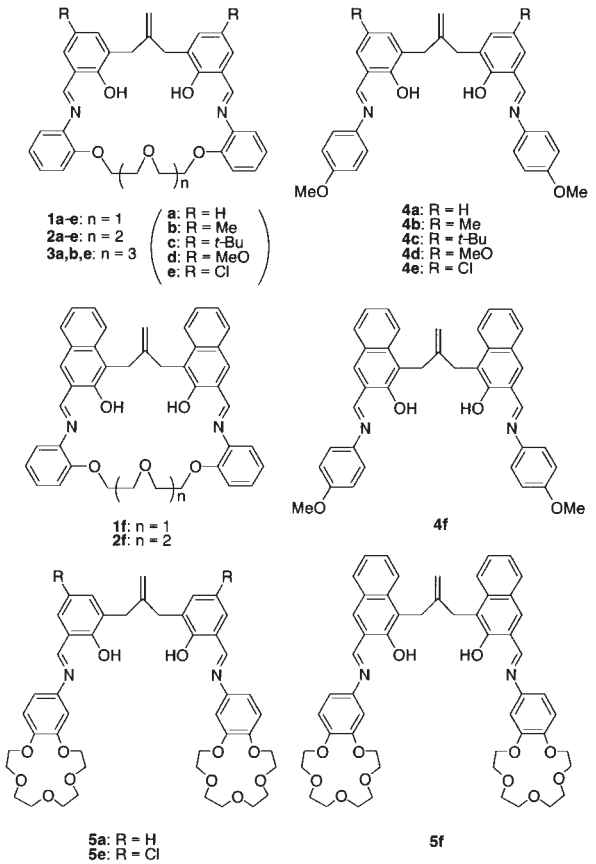

Fig. 2. Chemical structures of the imine compounds.

ray structure.[15] Utilizing the chart of the conformation–chemical shift relationship, we were able to follow the conformational change of a pincers-type crown ether derivative during its complexation with alkali metal ions. In that study, we also assumed that the isobutenylene chains of **1a**, **2a**, and **3a** (Fig. 2) adopt the *syn–syn* conformation, in spite of the lack of X-ray crystal structures for these compounds. However, the chemical shifts of these compounds were distributed in a wide range compared to the other groups of compounds, implying that the actual conformational population in solution sensitively reflects their chemical structure, namely the size of the macrocycle. Conversely, these compounds are good objects to examine the various factors affecting the conformational preference and magnetic shieldings of the isobutenylene chains. In this paper, we investigate a series of derivatives and analogues of **1a**, **2a**, and **3a** to clarify substituent effects and ring size effects on the actual conformational population.

Results and Discussion

Figure 2 shows the chemical structures of the compounds studied. The letters **a**–**f** denote the substituents on the phenyl ring of the salicylidene group. The length of the oxyethylene chain connecting the two aniline moieties in **1**–**3** is indicated by the compound number (**1**, $n = 1$; **2**, $n = 2$; **3**, $n = 3$; n is the number of the oxyethylene units). The compounds **4a**–**f**, **5a**, **5e**, and **5f** are acyclic analogues. Of these 24 compounds, we newly obtained the crystal structures of **2c**, **2f**, and **3b**. In the crystal structure of **2c** (Fig. 3a), a macrocycle with a

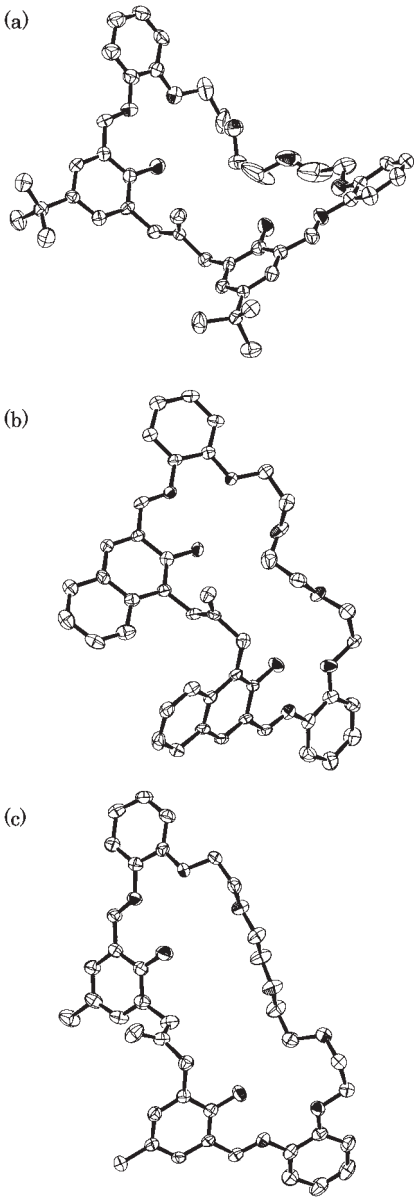

Fig. 3. Crystal structures of (a) **2c**, (b) **2f**, and (c) **3b**. The hydrogen atoms and the solvent(s) of crystallization are omitted for clarity.

triethylene glycol chain, the dihedral angles (ϕ_1, ϕ_2) are (3.3°, −3.3°); thus, the conformation of the isobutenylene chain was classified as *syn–syn*. The crystal structure of **2f** (Fig. 3b), in which the phenyl groups of **2c** are replaced by naphthalene moieties, revealed that the dihedral angles (ϕ_1, ϕ_2) of the isobutenylene chain are (6.2°, −140.0°). Thus, the conformation of the isobutenylene chain in **2f** was classified as the *syn*–skew. In the crystal structure of **3b** (Fig. 3c), a macrocycle with a tetraethylene glycol chain, the dihedral angles (ϕ_1, ϕ_2) of the isobutenylene chain are (8.7°, −110.7°), and the conformation of the isobutenylene chain was classified as the *syn*–skew.

To estimate the conformation of cyclophanes based on the magnetic shieldings caused by ring current effect is a well-known and established method.[16] Previously, we found that the chemical shifts (δH^a and δH^b) of the exo-methylene and

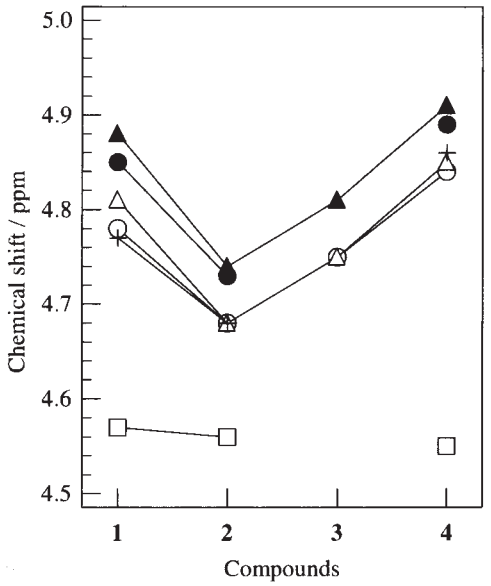

Fig. 4. Chemical shifts (δH^a) of imines **1**–**3** (open circles: **a** (R = H), open triangles: **b** (R = Me), crosses: **c** (R = *t*-Bu), solid circles: **d** (R = MeO), solid triangles: **e** (R = Cl), open squares: **f** (naphthalene)) as a function of size of the macrocycles (cf. Fig. 2). Acyclic imine **4** is included for reference.

benzylic protons (H^a and H^b in Fig. 1a) are a useful for identifying the conformation of the isobutenylene chain.[15] In the present study, we focused on H^a, which shows a relatively large change in chemical shift. Figure 4 shows the variation of δH^a as a function of the size of the macrocycle for the series of compounds **a**–**f** (**1**, **2**, and **3** have 24-, 27-, and 30-membered rings; cf. Fig. 2); acyclic compound **4** is included in Fig. 4 for reference. For series **a** (R = H), **b** (R = Me), and **c** (R = *t*-Bu), the plots are concave, with a minimum at **2**, and quite similar, indicating that the alkyl substituents hardly affect the δH^a value. Since the δH^a value is mainly determined by the conformation of the isobutenylene chain, these three series **a**–**c** of compounds **1**–**3** are conformationally similar in solution. For series **d** (R = MeO) and **e** (R = Cl), the plots are again similar. Moreover, these plots are similar to those for series **a**–**c**, but with an overall downfield shift of ~0.03 ppm. This downfield shift can be attributed to magnetic anisotropy effects of the oxygen or chlorine atoms. In contrast with the plots for series **a**–**e**, the plot for series **f** (naphthalene derivatives) is almost flat, showing only a slight dependence on the size of the macrocycle. The δH^a value of **2f** is 4.57 ppm, which is 0.11 ppm upfield of the δH^a value of **2a** (4.68 ppm).

The similarity of the values of the chemical shifts of **2a**–**e** (Fig. 4) indicates that the conformations of these compounds are likely to be similar irrespective of the substituent. According to our previous study, there is a fairly good correlation between the X-ray crystal structures and the solvated structures presumed from the ^{1}H NMR chemical shifts.[15] When the isobutenylene chain adopts the *syn* conformation, the exo-methylene proton (H^a) undergoes magnetic shielding by through-space effects, including the ring current effect and the γ-steric effect, resulting in an upfield shift of the resonance. Thus, the upfield-shifted δH^a of **2c** is consistent with its crystal structure, in which the isobutenylene chain adopts the *syn–syn* form. Accordingly, we suggest that the *syn–syn* conformer predominantly contributes to the structure of **2a**–**e** in solution. The δH^a values for **3a**–**e** fall between those of **2a**–**e** and those of the acyclic analogues **4a**–**e**, which have fewer constraints for conformational distribution, indicating that **3a**–**e** can move in the conformational space more freely than **2a**–**e** can. In view of the fact that **3b** adopts the *syn*–skew conformation in the crystal (Fig. 3c), the conformational distributions of **3a**–**e** may be biased toward the *syn*–skew form to some extent. In addition, the packing force in the crystal might have favored the *syn*–skew conformer. We suggest that the conformers of **1a**–**e**, like those of **3a**–**e**, are in equilibrium, with less contribution of the *syn–syn* form compared to the case for **2a**–**e**. Consequently, we can assume that the *syn–syn* conformer corresponds to a local potential minimum with relatively high energy, and that the triethylene glycol chain of **2a**–**e** has a length appropriate for stabilizing the *syn–syn* form.

For the compounds **1f**–**4f**, we observed only a slight change in δH^a with respect to the length of the linker moiety. There are two possible interpretations for the considerable substituent effects that occur when the phenyl groups are replaced by naphthalene moieties: (1) the equilibrium among the conformers does not depend on the molecular structure, that is, the size of the macrocycle; (2) the conformational dependence of the δH^a value is negligibly small. The assumption (1) is consistent with the fact that the isobutenylene chain of **2f** adopts the *syn*–skew form in the crystal (Fig. 3), even though **2f** has a triethylene glycol linkage, which could stabilize the *syn–syn* form. This result suggests that replacing the phenyl groups with naphthalene moieties destabilizes *syn–syn* conformer, and thereby **1f**–**4f** have similar conformational distributions with relatively low contributions of the *syn–syn* form. Disfavor of the *syn–syn* form is attributable to steric repulsion between the two naphthalene rings that are forced to be in proximity (cf. Fig. 1b). This assumption is supported by our preliminary ab initio molecular orbital calculation (MP2/6-311G**//HF/6-311G**),[17] which revealed that the relative energy (2.05 kcal/mol) of the *syn–syn* conformer with respect to the *syn*–skew conformer for a naphthalene derivative is nearly twice as high as that (1.21 kcal/mol) of the corresponding phenyl derivative. The large upfield shift of the resonance of **4f** (4.55 ppm) compared with that of **4a** (4.84 ppm) can be explained by the potentially strong ring current effect of the naphthalene group. On the other hand, the assumption (2) that the conformational dependence of the δH^a values is negligibly small seems hardly acceptable at once, since the naphthalene ring would exert stronger ring current effect. One possible case is that the H^a proton keeps undergoing strong ring current effects of the naphthalene rings all through the conformational change, resulting in the leveling of the δH^a values.

The assumption (2) can be disproved by observing an obvious change in δH^a by the conformational change. A benzo-15-crown-5-bearing compound such as **5a** is useful for examining the conformational dependence of δH^a, since it changes from a free-rotation state (equilibrium among three forms) to a skew–skew form upon addition of alkali metal ion (Fig. 5).[15] The ^{1}H NMR spectra of the chloro (**5e**) and naphthalene (**5f**) derivatives (Fig. 2) were measured before and after mixing

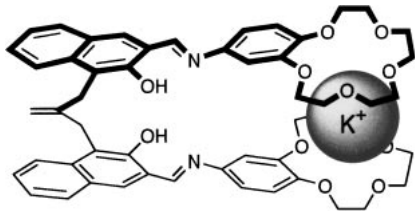

Fig. 5. Structure of the complex of **5f** and potassium ion.

Table 1. Chemical Shifts (ppm) of H^a before and after Addition of Potassium Ion

Compound	δH^a (without K^+)	δH^a (with K^+)	$\Delta\delta H^a$
5a[a)]	4.83	5.13	0.30
5e[b)]	4.90	5.19	0.29
5f[b)]	4.55	5.50	0.95

a) Ref. 15. b) This work.

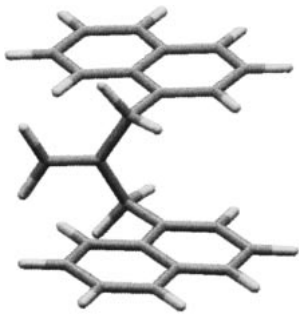

Fig. 6. Skew–skew conformer of 3-(1-naphthyl)-2-(1-naphthylmethyl)-1-propene as a model of the naphthalene derivatives of the isobutenylene-linked compounds.

with potassium tetrakis(3,5-bis(trifluoromethyl)phenyl)borate (K·TFPB). The binding constants $K = [\mathbf{5}\cdot K^+]/[\mathbf{5}][K^+]$ of **5a**, **5e**, and **5f** were estimated to be 8.2×10^3, 2.2×10^4, 3.6×10^3 M^{-1} (chloroform), respectively, from the titration experiments. Table 1 summarizes the H^a chemical shifts of **5a**, **5e**, and **5f** at free rotation, and those at K·TFPB-bound state. As shown in the last column of the table, the $\Delta\delta H^a$ values of **5a** and **5e** (0.30 and 0.29 ppm, respectively) are similar, whereas the $\Delta\delta H^a$ value of **5f** (0.95 ppm) is approximately three times as large as the $\Delta\delta H^a$ values of **5a** and **5e**. This difference suggests that the conformational dependence of δH^a of **5f** is larger than that expected from the second assumption in the previous paragraph. The large change in chemical shift can be explained by the relative geometry of the exo-methylene group and the naphthalene ring. A molecular modeling study[17] shows that, when one C=C–C–C moiety adopts the skew form, the H^a atom is located in the plane of the naphthalene ring (Fig. 6), resulting in a deshielding effect on H^a. Therefore, we conclude that the invariable chemical shift observed for the naphthalene derivatives is attributable not to the collapse of the conformation–chemical shift relationship, but to the change in conformational distribution, namely, the reduced population of the *syn–syn* form.

Through the above discussion, we stand on the assumption that the crystal structures are predominantly reflected in the structures in solution. In view of a clear correspondence between the crystal structure and chemical shift distribution observed for numbers of compounds, this assumption seems valid as far as the present series of compounds is concerned. Nevertheless, we found some exceptions: for example, **3b** is the *syn–*skew form with respect to the isobutenylene chain in the crystal, while the chemical shift suggests an equilibrium involving *syn–syn* forms in solution. We should note that the chemical shift is obtained as a thermodynamical average among several conformers even for the apparently rigid molecular systems, and should pay attention to such a case if the conformers with shallow potential minima are involved. For such cases, analyses of the temperature-dependence of the ^{1}H NMR spectra are potentially effective to identify the most stable conformer, though we confined our study to room-temperature experiments to accomplish our current purpose.

Conclusions

We have analyzed the ^{1}H NMR chemical shifts and crystal structures of several isobutenylene-linked Schiff bases in detail. We focused on compounds that were presumed to adopt the *syn–syn* conformation with respect to the isobutenylene chain in solution. X-ray crystal structure analysis revealed that one of these compounds adopts a *syn–syn* form, which validates the prediction based on the analysis of the ^{1}H NMR chemical shifts. The *syn–syn* conformer is not very preferable in a conformational space, and therefore its population in solution significantly depends on its molecular structure, especially the size of the macrocycle. Small substituents (*t*-butyl, methyl, methoxy, and chloro) on the phenyl ring hardly affected the stability of the *syn–syn* form, whereas replacement of phenyl groups with naphthalene moieties destabilized the *syn–syn* form. In a previous study,[15] we demonstrated the utility of the conformation–chemical shift relationship, particularly in monitoring the change in molecular conformation during supramolecular complexation. Our present results have shown that the conformation–chemical shift relationship is valid irrespective of substituent, including naphthalene, provided the conformational preference is correctly taken into account.

Experimental

The Schiff base compounds were prepared similarly to **1a**–**5a**:[15] the corresponding bis(hydroxybenzaldehyde) (0.5 mmol) and aniline derivative (0.5 mmol for diamine or 1.0 mmol for monoamine) were dissolved in chloroform (20 mL), and then methanol was gradually added over several days to allow a crystalline precipitate to separate out. The ^{1}H and ^{13}C NMR spectra were measured in $CDCl_3$ at 25 °C using a Bruker AVANCE500 (500 MHz for ^{1}H nuclei). ESI mass spectra were measured in the positive mode using a Waters 2690 system. The X-ray single crystal diffraction data were collected at −80 °C on a Rigaku RAXIS-RAPID imaging plate diffractometer (λ(Mo Kα) = 0.7107 Å). The structure was solved by direct methods and expanded using Fourier techniques. The non-hydrogen atoms were refined anisotropically. Hydrogen atoms' coordinates were calculated. The final cycle of full-matrix least-square refinement was based on the observed reflections of $I > 1.5\sigma(I)$ and the variable parameters, and converged with unweighted and weighted agreement factors R_1 and R_w. All calculations were performed using the teXsan crystallographic software package of Molecular Structure Corporation.[18] Crystallographic

data have been deposited at the CCDC, 12 Union Road, Cambridge CB2 1EZ, UK and copies can be obtained on request, free of charge, by quoting the publication citation and the deposition numbers 218388–218390.

Compound **1b**: ^{1}H NMR δ 2.28 (s, Ar–CH_3, 6H), 3.56 (s, Ar–CH_2–C(=CH$_2$)–, 4H), 4.07 (t, J = 5.0 Hz, Ar–O–CH$_2$–CH_2–O–, 4H), 4.18 (t, J = 4.9 Hz, Ar–O–CH_2–CH$_2$–O–, 4H), 4.81 (s, –C(=CH_2)–, 2H), 7.00 (d, J = 8.0 Hz, ArH, 2H), 7.01 (t, J = 8.0 Hz, ArH, 2H), 7.03 (d, J = 1.7 Hz, ArH, 2H), 7.07 (d, J = 1.8 Hz, ArH, 2H), 7.20 (t, J = 7.8 Hz, ArH, 2H), 7.24 (d, J = 7.8 Hz, ArH, 2H), 8.63 (s, Ar–CH=N–, 2H), 13.90 (s, Ar–OH, 2H). ^{13}C NMR δ 20.4, 35.9, 69.6, 70.6, 114.8, 118.1, 118.6, 121.7, 126.9, 127.7, 128.1, 129.9, 135.0, 137.8, 147.3, 152.7, 157.9, 161.0. ESI MS m/z 599.4 (calcd for M + Na$^+$: m/z 599.7). Elemental Analysis Found: C, 73.94; H, 6.11; N, 4.70%. Calcd for $C_{36}H_{36}N_2O_5\cdot(H_2O)_{0.5}$: C, 73.82; H, 6.37; N, 4.78%.

Compound **1c**: ^{1}H NMR δ 1.32 (s, Ar–C(CH_3)$_3$, 18H), 3.60 (s, Ar–CH_2–C(=CH$_2$)–, 4H), 4.08 (t, J = 4.9 Hz, Ar–O–CH$_2$–CH_2–O–, 4H), 4.18 (t, J = 4.9 Hz, Ar–O–CH_2–CH$_2$–O–, 4H), 4.77 (s, –C(=CH_2)–, 2H), 7.01 (d, J = 8.1 Hz, ArH, 2H), 7.02 (t, J = 8.1 Hz, ArH, 2H), 7.20 (t, J = 7.8 Hz, ArH, 2H), 7.23 (d, J = 2.5 Hz, ArH, 2H), 7.26 (d, J = 7.7 Hz, ArH, 2H), 7.32 (d, J = 2.5 Hz, ArH, 2H), 8.69 (s, Ar–CH=N–, 2H), 13.94 (s, Ar–OH, 2H). ^{13}C NMR δ 31.5, 34.0, 36.4, 69.7, 70.7, 111.2, 114.9, 118.1, 118.2, 121.8, 126.3, 127.7, 127.8, 131.7, 138.0, 140.6, 148.3, 152.8, 158.0, 161.4. ESI MS m/z 661.5 (calcd for M + H$^+$: m/z 661.8). Elemental Analysis Found: C, 75.69; H, 7.20; N, 4.16%. Calcd for $C_{42}H_{48}N_2O_5\cdot(H_2O)_{0.33}$: C, 75.64; H, 7.36; N, 4.20%.

Compound **1d**: ^{1}H NMR δ 3.57 (s, Ar–CH_2–C(=CH$_2$)–, 4H), 3.79 (s, Ar–OCH_3, 6H), 4.08 (t, J = 5.0 Hz), Ar–O–CH$_2$–CH_2–O–, 4H), 4.18 (t, J = 5.0 Hz), Ar–O–CH_2–CH$_2$–O–, 4H), 4.85 (s, –C(=CH_2)–, 2H), 6.75 (d, J = 3.1 Hz, ArH, 2H), 6.91 (d, J = 3.1 Hz, ArH, 2H), 7.00 (d, J = 7.9 Hz, ArH, 2H), 7.01 (t, J = 7.9 Hz, ArH, 2H), 7.21 (t, J = 7.5 Hz, ArH, 2H), 7.25 (d, J = 7.5 Hz, ArH, 2H), 8.65 (s, Ar–CH=N–, 2H), 13.74 (s, Ar–OH, 2H). ^{13}C NMR δ 36.0, 55.9, 69.6, 70.6, 112.6, 114.7, 118.1, 121.6, 121.7, 127.9, 129.7, 137.6, 147.6, 151.5, 152.7, 154.7, 160.6. ESI MS m/z 609.4 (calcd for M + H$^+$: m/z 609.7). Elemental Analysis Found: C, 70.55; H, 5.82; N, 4.49%. Calcd for $C_{36}H_{36}N_2O_7\cdot(H_2O)_{0.25}$: C, 70.51; H, 6.00; N, 4.57%.

Compound **1e**: ^{1}H NMR δ 3.55 (s, Ar–CH_2–C(=CH$_2$)–, 4H), 4.07 (t, J = 5.0 Hz, Ar–O–CH$_2$–CH_2–O–, 4H), 4.19 (t, J = 5.0 Hz, Ar–O–CH_2–CH$_2$–O–, 4H), 4.88 (s, –C(=CH_2)–, 2H), 6.99 (d, J = 7.1 Hz, ArH, 2H), 7.02 (t, J = 7.6 Hz, ArH, 2H), 7.19 (d, J = 2.6 Hz, ArH, 2H), 7.21 (t, J = 2.6 Hz, ArH, 2H), 7.23 (t, J = 7.7 Hz, ArH, 2H), 7.26 (d, J = 7.8 Hz, ArH, 2H), 8.62 (s, Ar–CH=N–, 2H), 14.31 (s, Ar–OH, 2H). ^{13}C NMR δ 35.7, 69.3, 70.5, 114.4, 118.0, 119.6, 121.7, 122.7, 128.4, 128.9, 130.5, 133.3, 158.8, 159.2. ESI MS m/z 617.4 (calcd for M + H$^+$: m/z 617.6). Elemental Analysis Found: C, 65.45; H, 4.69; N, 4.38%. Calcd for $C_{34}H_{30}Cl_2N_2O_5\cdot(H_2O)_{0.33}$: C, 65.49; H, 4.96; N, 4.49%.

Compound **1f**: ^{1}H NMR δ 4.10 (s, Ar–CH_2–C(=CH$_2$)–, 4H), 4.20–26 (m, Ar–O–CH_2–CH_2–O–, 8H), 4.57 (s, –C(=CH_2)–, 2H), 7.04 (d, J = 8.1 Hz, ArH, 2H), 7.06 (t, J = 7.8 Hz, ArH, 2H), 7.26 (t, J = 8.0 Hz, ArH, 2H), 7.29 (t, J = 8.0 Hz, ArH, 2H), 7.40 (d, J = 7.8 Hz, ArH, 2H), 7.47 (t, J = 7.6 Hz, ArH, 2H), 7.80 (d, J = 8.1 Hz, ArH, 2H), 7.83 (d, J = 8.7 Hz, ArH, 2H), 7.88 (s, ArH, 2H), 8.91 (s, Ar–CH=N–, 2H), 13.99 (s, Ar–OH, 2H). The ^{13}C NMR spectrum was not measured owing to low solubility. ESI MS m/z 649.5 (calcd for M + Na$^+$ m/z 649.7). Elemental Analysis Found: C, 76.79; H, 5.40; N, 4.08%. Calcd for $C_{42}H_{36}N_2O_5\cdot(H_2O)_{0.5}$: C, 76.69; H, 5.67; N, 4.26%.

Compound **2b**: ^{1}H NMR δ 2.30 (s, Ar-CH_3, 6H), 3.50 (s, Ar–CH_2–C(=CH$_2$)–, 4H), 3.92 (s, Ar–O–CH_2–CH_2–O–Ar, 4H), 3.92 (t, J = 3.9 Hz, Ar–O–CH$_2$–CH_2–O–, 4H), 4.16 (t, J = 3.9 Hz, Ar–O–CH_2–CH$_2$–O–, 4H), 4.68 (s, –C(=CH_2)–, 2H), 6.92 (d, J = 8.2 Hz, ArH, 2H), 6.98 (t, J = 8.0 Hz, ArH, 2H), 7.06 (m, ArH, 4H), 7.20 (t, J = 8.0 Hz, ArH, 2H), 7.23 (d, J = 8.0 Hz, ArH, 2H), 8.64 (s, Ar–CH=N–, 2H), 13.99 (s, Ar–OH, 2H). ^{13}C NMR δ 20.4, 35.9, 69.5, 69.9, 72.0, 110.4, 112.7, 117.9, 118.7, 121.0, 127.0, 127.8, 130.0, 135.1, 137.1, 148.7, 152.8, 157.7, 160.8. ESI MS m/z 643.3 (calcd for M + Na$^+$: m/z 643.7). Elemental Analysis Found: C, 72.95; H, 6.42; N, 4.40%. Calcd for $C_{38}H_{40}N_2O_6\cdot(H_2O)_{0.25}$: C, 73.00; H, 6.53; N, 4.48%.

Compound **2c**: ^{1}H NMR δ 1.33 (s, Ar–C(CH_3)$_3$, 18H), 3.54 (s, Ar–CH_2–C(=CH$_2$)–, 4H), 3.93 (s, Ar–O–CH_2–CH_2–O–Ar, 4H), 3.93 (t, J = 4.0 Hz, Ar–O–CH$_2$–CH_2–O–, 4H), 4.16 (t, J = 4.0 Hz, Ar–O–CH_2–CH$_2$–O–, 4H), 4.68 (s, –C(=CH_2)–, 2H), 6.92 (d, J = 8.1 Hz, ArH, 2H), 6.99 (t, J = 8.1 Hz, ArH, 2H), 7.20 (t, J = 7.8 Hz, ArH, 2H), 7.23–26 (m, ArH, 4H), 7.29 (d, J = 2.5 Hz, ArH, 2H), 8.69 (s, Ar–CH=N–, 2H), 13.97 (s, Ar–OH, 2H). ^{13}C NMR δ 31.5, 34.0, 36.3, 69.6, 69.9, 72.1, 110.5, 112.7, 117.9, 118.3, 121.0, 126.4, 127.5, 127.7, 131.9, 137.4, 140.6, 148.6, 152.8, 157.8, 161.3. ESI MS m/z 727.5 (calcd for M + Na$^+$: m/z 727.9). Elemental Analysis Found: C, 65.69; H, 6.52; N, 3.31%. Calcd for $C_{44}H_{52}N_2O_6\cdot CHCl_3$: C, 65.57; H, 6.48; N, 3.40%.

Crystal data for **2c**: $C_{45}H_{53}N_2O_6Cl_3$, MW = 824.28, crystal system = orthorhombic, space group $P2_1/n2_1/m2_1/a$ (#62), Z = 4 in a cell of dimensions: a = 25.7433(3), b = 30.4536(4), c = 5.5793(1) Å, V = 4374.06(10) Å^3, D_{calcd} = 1.252 g/cm^3. μ = 2.57/cm, 36591 measured and 5112 unique reflections ($2\theta_{max}$ = 55.0°, R_{int} = 0.055). R_1 = 0.066, R_w = 0.121. The C23–C23* bond is extremely short (1.029 Å). In view of the large anisotropy of this carbon atom, we conclude that this short bond is due to the conformational disorder of the ethylene glycol chain.

Compound **2d**: ^{1}H NMR δ 3.51 (s, Ar–CH_2–C(=CH$_2$)–, 4H), 3.80 (s, Ar–OCH_3, 6H), 3.93 (s, Ar–O–CH_2–CH_2–O–Ar, 4H), 3.94 (t, J = 4.1 Hz, Ar–O–CH$_2$–CH_2–O–, 4H), 4.17 (t, J = 4.1 Hz, Ar–O–CH_2–CH$_2$–O–, 4H), 4.73 (s, –C(=CH_2)–, 2H), 6.78 (d, J = 3.1 Hz, ArH, 2H), 6.90 (t, J = 3.1 Hz, ArH, 2H), 6.92 (d, J = 7.3 Hz, ArH, 2H), 6.99 (t, J = 7.6 Hz, ArH, 2H), 7.21 (t, J = 8.3 Hz, ArH, 2H), 7.25 (d, J = 7.9 Hz, ArH, 2H), 8.65 (s, Ar–CH=N–, 2H), 13.78 (s, Ar–OH, 2H). ^{13}C NMR δ 36.0, 55.9, 69.5, 69.9, 72.0, 112.7, 113.0, 117.9, 118.6, 121.0, 121.6, 128.0, 129.3, 137.0, 147.9, 151.5, 152.8, 154.5, 160.5. ESI MS m/z 675.4 (calcd for M + Na$^+$: m/z 675.7). Elemental Analysis Found: C, 68.90; H, 6.01; N, 4.13%. Calcd for $C_{38}H_{40}N_2O_8\cdot(H_2O)_{0.5}$: C, 68.97; H, 6.25; N, 4.23%.

Compound **2e**: ^{1}H NMR δ 3.49 (s, Ar–CH_2–C(=CH$_2$)–, 4H), 3.92 (s, –O–CH_2–CH_2–O–, 4H), 3.94 (t, J = 4.1 Hz, Ar–O–CH$_2$–CH_2–O–, 4H), 4.18 (t, J = 4.1 Hz, Ar–O–CH_2–CH$_2$–O–, 4H), 4.74 (s, –C(=CH_2)–, 2H), 6.93 (d, J = 8.3 Hz, ArH, 2H), 7.00 (t, J = 7.7 Hz, ArH, 2H), 7.20 (d, J = 2.6 Hz, ArH, 2H), 7.22–26 (m, ArH, 6H), 8.63 (s, Ar–CH=N–, 2H), 14.32 (s, Ar–OH, 2H). ^{13}C NMR δ 35.7, 69.4, 69.9, 72.0, 111.9, 112.7, 117.9, 119.8, 121.1, 122.7, 128.5, 129.0, 130.0, 133.5, 136.2, 146.9, 152.8, 158.6, 159.3. ESI MS m/z 683.4 (calcd for M + Na$^+$: m/z 683.6). Elemental Analysis Found: C, 65.25; H, 5.10; N, 4.11%. Calcd for $C_{36}H_{34}Cl_2N_2O_6$: C, 65.35; H, 5.18; N, 4.24%.

Compound **2f**: ^{1}H NMR δ 4.00 (t, J = 4.1 Hz, Ar–O–CH$_2$–CH_2–O–, 4H), 4.05 (s, Ar–CH_2–C(=CH$_2$)–, 4H), 4.08 (s, –O–CH_2–CH_2–O–, 4H), 4.22 (t, J = 4.1 Hz, Ar–O–CH_2–CH$_2$–O–,

4H), 4.56 (s, –C(=CH_2)–, 2H), 6.96 (d, J = 8.2 Hz, ArH, 2H), 7.03 (t, J = 7.6 Hz, ArH, 2H), 7.26 (t, J = 7.9 Hz, ArH, 2H), 7.29 (t, J = 7.2 Hz, ArH, 2H), 7.33 (d, J = 7.8 Hz, ArH, 2H), 7.39 (t, J = 7.7 Hz, ArH, 2H), 7.72 (d, J = 8.6 Hz, ArH, 2H), 7.80 (d, J = 7.8 Hz, ArH, 2H), 7.89 (s, ArH, 2H), 8.87 (s, Ar–CH=N–, 2H), 13.78 (s, Ar–OH, 2H). The ^{13}C NMR spectrum was not measured owing to low solubility. ESI MS m/z 693.5 (calcd for M + H^+: m/z 693.8). Elemental Analysis Found: C, 74.86; H, 5.70; N, 3.82%. Calcd for $C_{44}H_{40}N_2O_6 \cdot (H_2O)_{0.67}$: C, 74.97; H, 5.91; N, 3.98%.

Crystal data for **2f**: $C_{46.5}H_{43}Cl_{7.5}N_2O_6$, MW = 991.76, crystal system = triclinic, space group $P\bar{1}$ (#2), Z = 2 in a cell of dimensions: a = 17.0224(5), b = 17.5847(3), c = 9.1478(1) Å, α = 95.816(2), β = 102.718(3), γ = 117.858(1)°, V = 2294.4(1) Å^3, D_{calcd} = 1.435 g/cm^3. μ = 5.12/cm, 19821 measured and 9728 unique reflections ($2\theta_{max}$ = 55.0°, R_{int} = 0.045). R_1 = 0.119, R_w = 0.240. The non-integral composition is a result of counting half of the chloroform molecule. This chloroform molecule is located around the crystallographic inversion point and is disordered with respect to its direction. The rather high R values seem to be attributable to this disorder.

Compound **3b**: ^{1}H NMR δ 2.30 (s, Ar–CH_3, 6H), 3.50 (s, Ar–CH_2–C(=CH$_2$)–, 4H), 3.70 (t, J = 4.9 Hz, –O–CH_2–CH$_2$–O–, 4H), 3.82 (t, J = 4.9 Hz, –O–CH$_2$–CH_2–O–, 4H), 3.92 (t, J = 4.1 Hz, Ar–O–CH$_2$–CH_2–O–, 4H), 4.16 (t, J = 4.1 Hz, Ar–O–CH_2–CH$_2$–O–, 4H), 4.75 (s, –C(=CH_2)–, 2H), 6.93 (d, J = 8.3 Hz, ArH, 2H), 6.99 (t, J = 7.6 Hz, ArH, 2H), 7.06–07 (m, ArH, 4H), 7.18–23 (m, ArH, 4H), 8.65 (s, Ar–CH=N–, 2H), 13.82 (s, Ar–OH, 2H). ^{13}C NMR δ 20.4, 35.6, 69.1, 69.6, 70.5, 70.9, 111.5, 112.8, 118.5, 118.8, 121.1, 127.1, 127.5, 127.7, 130.2, 134.9, 137.5, 148.1, 152.5, 157.6, 161.5. ESI MS m/z 687.5 (calcd for M + H^+: m/z 687.8). Elemental Analysis Found: C, 72.27; H, 6.65; N, 4.05%. Calcd for $C_{40}H_{44}N_2O_7$: C, 72.27; H, 6.67; N, 4.21%.

Crystal data for **3b**: $C_{40}H_{44}N_2O_7$, MW = 664.80, crystal system = orthorhombic, space group $Pca2_1$ (#29), Z = 4 in a cell of dimensions: a = 8.6766(2), b = 21.9579(5), c = 18.5332(4) Å, V = 3530.9(3) Å^3, D_{calcd} = 1.250 g/cm^3. μ = 0.85/cm, 29392 measured and 4179 unique reflections ($2\theta_{max}$ = 55.0°, R_{int} = 0.051). R_1 = 0.042, R_w = 0.080.

Compound **3e**: ^{1}H NMR δ 3.48 (s, Ar–CH_2–C(=CH$_2$)–, 4H), 3.71 (t, J = 5.0 Hz, –O–CH_2–CH$_2$–O–, 4H), 3.80 (t, J = 5.0 Hz, –O–CH$_2$–CH_2–O–, 4H), 3.92 (t, J = 4.1 Hz, Ar–O–CH$_2$–CH_2–O–, 4H), 4.16 (t, J = 4.1 Hz, Ar–O–CH_2–CH$_2$–O–, 4H), 4.81 (s, –C(=CH_2)–, 2H), 6.93 (d, J = 8.4 Hz, ArH, 2H), 6.99 (t, J = 7.6 Hz, ArH, 2H), 7.20 (d, J = 2.6 Hz, ArH, 2H), 7.22–26 (m, ArH, 6H), 8.65 (s, Ar–CH=N–, 2H), 14.18 (s, Ar–OH, 2H). ^{13}C NMR δ 35.8, 69.4, 70.1, 71.0, 71.3, 113.2, 119.0, 120.3, 121.4, 121.6, 123.2, 128.8, 129.5, 130.2, 133.6, 136.8, 146.7, 153.0, 158.9, 160.3. ESI MS m/z 727.4 (calcd for M + Na^+: m/z 727.7). Elemental Analysis Found: C, 64.35; H, 5.29; N, 3.84%. Calcd for $C_{38}H_{38}Cl_2N_2O_7$: C, 64.68; H, 5.43; N, 3.97%.

Compound **4b**: ^{1}H NMR δ 2.29 (s, Ar–CH_3, 6H), 3.49 (s, Ar–CH_2–C(=CH$_2$)–, 4H), 3.84 s, Ar–O–CH_3, 6H), 4.85 (s, –C(=CH_2)–, 2H), 6.93 (d, J = 9.0 Hz, ArH, 2H), 7.04 (d, J = 1.7 Hz, ArH, 2H), 7.10 (d, J = 1.7 Hz, ArH, 2H), 7.25 (d, J = 9.0 Hz, ArH, 4H), 8.55 (s, Ar–CH=N–, 2H), 13.47 (s, Ar–OH, 2H). ^{13}C NMR δ 20.4, 35.8, 55.5, 112.2, 114.5, 118.5, 121.2, 127.3, 127.5, 130.2, 134.9, 141.6, 157.0, 158.6, 160.6. ESI MS m/z 557.4 (calcd for M + Na^+: m/z 557.6). Elemental Analysis Found: C, 76.36; H, 6.32; N, 5.17%. Calcd for $C_{34}H_{34}N_2O_4$: C, 76.38; H, 6.41; N, 5.24%.

Compound **4c**: ^{1}H NMR δ 1.33 (s, Ar–C(CH_3)$_3$, 18H), 3.52 (s, Ar–CH_2–C(=CH$_2$)–, 4H), 3.84 (s, Ar–O–CH_3, 6H), 4.86 (s, –C(=CH_2)–, 2H), 6.94 (d, J = 9.0 Hz, ArH, 2H), 7.24 (d, J = 2.5 Hz, ArH, 2H), 7.27 (d, J = 9.0 Hz, ArH, 4H), 7.36 (d, J = 2.5 Hz, ArH, 2H), 8.62 (s, Ar–CH=N–, 2H), 13.52 (s, Ar–OH, 2H). ^{13}C NMR δ 31.5, 34.0, 36.0, 55.5, 112.4, 114.6, 118.1, 122.2, 126.6, 127.0, 131.5, 141.1, 141.7, 147.0, 157.0, 158.6, 161.1. ESI MS m/z 641.5 (calcd for M + Na^+: m/z 641.8). Elemental Analysis Found: C, 77.48; H, 7.47; N, 4.40%. Calcd for $C_{40}H_{46}N_2O_4$: C, 77.64; H, 7.49; N, 4.53%.

Compound **4d**: ^{1}H NMR δ 3.50 (s, Ar–CH_2–C(=CH$_2$)–, 4H), 3.79 (s, Ar–OCH_3, 6H), 3.85 (s, Ar–O–CH_3, 6H), 4.89 (s, –C(=CH_2)–, 2H), 6.76 (d, J = 3.1 Hz, ArH, 2H), 6.93 (d, J = 8.9 Hz, ArH, 2H), 6.94 (d, J = 3.1 Hz, ArH, 2H), 7.25 (d, J = 9.0 Hz, ArH, 4H), 8.56 (s, Ar–CH=N–, 2H), 13.25 (s, Ar–OH, 2H). ^{13}C NMR δ 35.9, 55.5, 55.9, 113.5, 114.6, 118.5, 120.9, 122.3, 128.8, 141.5, 151.8, 153.6, 158.8, 160.3. ESI MS m/z 567.4 (calcd for M + H^+: m/z 567.6). Elemental Analysis Found: C, 72.23; H, 6.00; N, 4.92%. Calcd for $C_{34}H_{34}N_2O_6$: C, 72.06; H, 6.05; N, 4.95%.

Compound **4e**: ^{1}H NMR δ 3.47 (s, Ar–CH_2–C(=CH$_2$)–, 4H), 3.84 (s, Ar–O–CH_3, 6H), 4.91 (s, –C(=CH_2)–, 2H), 6.93 (d, J = 8.9 Hz, ArH, 2H), 7.20 (d, J = 2.6 Hz, ArH, 2H), 7.22 (d, J = 2.6 Hz, ArH, 2H), 7.25 (d, J = 9.0 Hz, ArH, 2H), 8.51 (s, Ar–CH=N–, 2H), 13.74 (s, Ar–OH, 2H). ^{13}C NMR δ 35.5, 55.5, 113.8, 114.7, 119.6, 122.4, 123.2, 129.1, 129.5, 133.2, 140.8, 145.6, 157.8, 159.0. ESI MS m/z 575.3 (calcd for M + H^+: m/z 575.6). Elemental Analysis Found: C, 66.91; H, 4.77; N, 4.79%. Calcd for $C_{32}H_{28}Cl_2N_2O_4$: C, 66.78; H, 4.90; N, 4.87%.

Compound **4f**: ^{1}H NMR δ 3.86 (s, Ar–O–CH_3, 6H), 4.08 (s, Ar–CH_2–C(=CH$_2$)–, 4H), 4.55 (s, –C(=CH_2)–, 2H), 6.97 (d, J = 8.9 Hz, ArH, 4H), 7.29 (t, J = 7.5 Hz, ArH, 2H), 7.34 (d, J = 8.9 Hz, ArH, 4H), 7.41 (t, J = 7.7 Hz, ArH, 2H), 7.79 (d, J = 7.5 Hz, ArH, 2H), 7.81 (d, J = 8.1 Hz, ArH, 2H), 7.86 (s, ArH, 2H), 8.79 (s, Ar–CH=N–, 2H), 13.26 (s, Ar–OH, 2H). The ^{13}C NMR spectrum was not measured owing to low solubility. ESI MS m/z 607.5 (calcd for M + H^+: m/z 607.7). Elemental Analysis Found: C, 77.49; H, 5.30; N, 4.30%. Calcd for $C_{40}H_{34}N_2O_4 \cdot (H_2O)_{0.67}$: C, 77.64; H, 5.76; N, 4.53%.

Compound **5e**: ^{1}H NMR δ 3.47 (s, Ar–CH_2–C(=CH$_2$)–, 4H), 3.76–78 (m, –O–CH_2–CH_2–O–, 16H), 3.92–94 (m, –O–CH_2–CH_2–O–, 8H), 4.16–18 (m, –O–CH_2–CH_2–O–, 8H), 4.90 (s, –C(=CH_2)–, 2H), 6.85–90 (m, ArH, 6H), 7.21 (d, J = 2.6 Hz, ArH, 2H), 7.23 (d, J = 2.6 Hz, ArH, 2H), 8.51 (s, Ar–CH=N–, 2H), 13.72 (s, Ar–OH, 2H). ^{13}C NMR δ 35.6, 69.0, 69.3, 69.5, 69.6, 70.5, 70.5, 71.1, 107.7, 113.4, 113.7, 114.3, 119.5, 123.2, 129.2, 129.6, 133.3, 141.5, 145.5, 148.8, 149.8, 157.8, 159.3. ESI MS m/z 895.5 (calcd for M + H^+: m/z 895.9). Elemental Analysis Found: C, 61.13; H, 5.76; N, 2.98%. Calcd for $C_{46}H_{52}Cl_2N_2O_{12} \cdot (H_2O)_{0.5}$: C, 61.06; H, 5.90; N, 3.10%.

Compound **5f**: ^{1}H NMR δ 3.76–80 (m, –O–CH_2–CH_2–O–, 16H), 3.93–96 (m, –O–CH_2–CH_2–O–, 8H), 4.08 (s, Ar–CH_2–C(=CH$_2$)–, 4H), 4.17–21 (m, –O–CH_2–CH_2–O–, 8H), 4.55 (s, –C(=CH_2)–, 2H), 6.91–96 (m, ArH, 6H), 7.29 (t, J = 7.4 Hz, ArH, 2H), 7.41 (t, J = 7.7 Hz, ArH, 2H), 7.79 (d, J = 7.0 Hz, ArH, 2H), 7.80 (d, J = 8.7 Hz, ArH, 2H), 7.87 (s, ArH, 2H), 8.77 (s, Ar–CH=N–, 2H), 13.22 (s, Ar–OH, 2H). ^{13}C NMR δ 31.7, 69.0, 69.3, 69.5, 69.6, 70.5, 70.5, 71.1, 107.8, 113.4, 114.3, 119.1, 121.0, 123.1, 123.8, 127.6, 128.2, 129.1, 132.9, 135.4, 142.0, 146.5, 148.6, 149.7, 154.5, 160.7. ESI MS m/z 927.6 (calcd for M + H^+: m/z 928.0). Elemental Analysis Found: C, 69.15; H, 6.21; N, 2.86%. Calcd for $C_{54}H_{58}N_2O_{12} \cdot (H_2O)_{0.5}$: C, 69.29; H, 6.35; N, 2.99%.

References

1 P. Guerriero, S. Tamburini, and P. A. Vigato, *Coord. Chem. Rev.*, **139**, 17 (1995).

2 T. R. Youkin, E. F. Connor, J. I. Henderson, S. K. Friedrich, R. H. Grubbs, and D. A. Bansleben, *Science*, **287**, 460 (2000).

3 S. Matsui, M. Mitani, J. Saito, N. Matsukawa, H. Tanaka, T. Nakano, and T. Fujita, *Chem. Lett.*, **2000**, 554.

4 C. F. Works and P. C. Ford, *J. Am. Chem. Soc.*, **122**, 7592 (2000).

5 Y. Shao, Y. Qiu, X. Hu, and X. Hong, *Chem. Lett.*, **2000**, 1068.

6 S. R. Korupoju, N. Mangayarkarasi, S. Ameerunisha, E. J. Valente, and P. S. Zacharias, *J. Chem. Soc., Dalton Trans.*, **2000**, 2845.

7 S. Akine, T. Taniguchi, and T. Nabeshima, *Tetrahedron Lett.*, **42**, 8861 (2001).

8 H. Shimakoshi, T. Kai, I. Aritome, and Y. Hisaeda, *Tetrahedron Lett.*, **43**, 8261 (2002).

9 M. Albrecht, *Chem. Rev.*, **101**, 3457 (2001).

10 M. L. N. Rao, H. Houjou, and K. Hiratani, *Chem. Commun.*, **2002**, 420.

11 M. Kanesato, H. Houjou, Y. Nagawa, and K. Hiratani, *Inorg. Chem. Commun.*, **5**, 984 (2002).

12 H. Houjou, A. Iwasaki, T. Ogihara, M. Kanesato, S. Akabori, and K. Hiratani, *New J. Chem.*, **27**, 886 (2003).

13 S. Tsuzuki, H. Houjou, Y. Nagawa, and K. Hiratani, *J. Chem. Soc., Perkin Trans. 2*, **2000**, 2448.

14 K. Hiratani, J. Suga, Y. Nagawa, H. Houjou, H. Tokuhisa, M. Numata, and K. Watanabe, *Tetrahedron Lett.*, **43**, 5747 (2002).

15 H. Houjou, S. Tsuzuki, Y. Nagawa, and K. Hiratani, *Bull. Chem. Soc. Jpn.*, **75**, 831 (2002).

16 Y. Fukazawa, K. Ogata, and S. Usui, *J. Am. Chem. Soc.*, **110**, 8692 (1988).

17 An ab initio study on 3-(1-naphthyl)-2-(1-naphthylmethyl)-1-propene is now in progress by H. Houjou, S. Tsuzuki, Y. Nagawa, M. Kanesato, and K. Hiratani.

18 "teXsan: Crystal Structure Analysis Package," Molecular Structure Corporation, Woodland, TX, USA (1985 & 1999).